New Concepts at the Interface: Novel Viewpoints and Interpretations, Theory and Computations

Directional and Rotational Motions of Nanoparticles on Plasma Membranes as Local Probes of Surface Tension Propagation

Shixin Li, Zengshuai Yan, Zhen Luo, Yan Xu, Fang Huang, Guoqing Hu, Xianren Zhang, and Tongtao Yue

Langmuir, **Just Accepted Manuscript** • Publication Date (Web): 25 Mar 2019

Directional and Rotational Motions of Nanoparticles on Plasma Membranes as Local Probes of Surface Tension Propagation

Shixin Li,[†] Zengshuai Yan,[‡] Zhen Luo,[‡] Yan Xu,[‡] Fang Huang,[†] Guoqing Hu,[*,∥,§] Xianren Zhang,[⊥] and Tongtao Yue[*,†,‡]

[†]State Key Laboratory of Heavy Oil Processing, China University of Petroleum (East China), Qingdao 266580, China

[‡]Center for Bioengineering and Biotechnology, College of Chemical Engineering, China University of Petroleum (East China), Qingdao 266580, China

[∥]State Key Laboratory of Nonlinear Mechanics (LNM), Institute of Mechanics, Chinese Academy of Science, Beijing 100190, China

[§]School of Engineering Science, University of Chinese Academy of Sciences, Beijing 100049, China

[⊥] State Key Laboratory of Organic-Inorganic Composites, Beijing University of Chemical Technology, Beijing 100029, China

ABSTRACT: Mechanical heterogeneity is ubiquitous in plasma membranes and of essential importance to cellular functioning. As a feedback of mechanical stimuli, local surface tension can be readily changed and immediately propagated through the membrane, influencing structures and dynamics of both inclusions and membrane associated proteins. Using the non-equilibrium coarse-grained membrane simulation, here we investigate the interrelated processes of tension propagation, lipid diffusion, and transport of nanoparticles (NPs) adhering on the membrane of constant tension gradient, mimicking that of migrating cells or cells under prolonged stimulation. Our results demonstrate that the lipid bilayer membrane can by itself propagate surface tension in defined rates and pathways to reach a dynamic equilibrium state where surface tension is linearly distributed along the gradient maintained by the directional flow-like motion of lipids. Such lipid flow exerts shearing forces to transport adhesive NPs toward the region of a larger surface tension. Under certain conditions, the shearing force can generate nonzero torques driving the rotational motion of NPs, with the direction of the NP rotation determined by the NP-membrane interaction state as functions of both the NP property and the local membrane surface tension. Such features endow NPs with promising applications ranging from biosensing to targeted drug delivery.

KEYWORDS: *plasma membrane, surface tension propagation, nanoparticle, rotation, dissipative particle dynamics*

INTRODUCTION

The plasma membrane, which represents a physical barrier segregating the interior of cells from the extracellular space, is made up of different types of lipids and proteins. The compositional complexity readily generates both structural and mechanical heterogeneities of the membrane,[1, 2] being essential to a wide range of cellular processes, such as cell migration,[3-5] endocytosis,[6, 7] and signaling.[8, 9] In particular, the membrane surface tension can locally change in response to external stimuli and orchestrates complex aspects of trafficking and motility.[10] For instance, the membrane surface tension was measured persistently ~30% higher at the leading edge than at the trailing edge of migrating cells.[11] Polymerization or contraction of actin associated with the membrane respectively induces an increase or a decrease of the local surface tension.[6, 12] Once changed, it serves as a stimulus for activation of mechanosensitive membrane-embedded ion channels,[13] or it could be released *via* programmed membrane trafficking events, such as budding and vesicle fusion.[14, 15] More recently, it was evidenced that nanometer-short stress pulses can be efficiently propagated through lipid bilayers to reach length scales up to tens of nanometers before attenuation.[16] Similar behaviors of 2D pressure pulse propagation in lipid monolayers were directly observed in experiments,[17] manifesting that the locally changed surface tension can be propagated through the membrane in defined rates and pathways. However, to the best of our knowledge, there is no literature reporting the surface tension propagation through membranes of persistent tension gradient, which is one important aspect of migrating cells or cells under prolonged stimulation.[4, 11]

The dynamics of surface tension propagation affects localization and movement of membrane inclusions that impact signaling and trafficking events involved. Engineered NPs, owing to their varying physicochemical properties, are increasingly considered as simplified models of proteins for exploring biological activities on plasma membranes.[18] Besides, understanding and control of the transport of NPs on plasma membranes are essential to their biomedical applications, ranging from biosensing to drug delivery.[19-29] In the past decades, both experimental and

computational efforts have been made in elucidation of the molecular mechanisms controlling interactions between NPs and plasma membranes.[23, 24, 27, 30-33] However, nearly all these previous studies have ignored the impact of mechanical heterogeneity, which is ubiquitous and an important aspect of real plasma membranes. Here we present the first computational investigation on the interrelated processes of surface tension propagation, lipid diffusion, and transport of NPs on the plasma membrane, mimicking that of migrating cells or the cells under constant mechanical stimulation.[11, 34] Our results show that surface tension is able to propagate efficiently through the membrane to reach a linear distribution along the gradient. The flow-like motion of lipids will exert shearing forces on the adhesive NPs to drive a directional transport toward the region of a larger surface tension. Moreover, the shearing forces can generate non-zero torques to induce a rotational motion of NPs, with direction and speed of the NP rotation determined by the NP-membrane interactions.

Notably, both translational and rotational motions of NPs have recently become detectable using 4D electron microscopy with high temporal and spatial resolutions.[35] By offering a molecular-level interpretation of the complex transport of NPs on the plasma membrane of mechanical heterogeneity, our results may provide guidelines answering what properties of NPs should be tuned to regulate the membrane interaction state and achieve a quantitative control of transport of NPs on plasma membranes.

EXPERIMENTAL SECTION

Models. In this system, each lipid molecule was coarse grained into three hydrophilic beads (H) connecting with two tails, each containing five hydrophobic beads (T) (Figure 1a). This coarse-grained model was proposed by Groot and Rabone and proved to show typical phase behaviors of the lipid bilayer.[36] Each NP was constructed by arranging a number of hydrophilic beads (P) into a spherical shape with a diameter of 8.0 nm, and was restrained to move as a rigid body during the simualtion (Figure 1b). Water molecules, which were modeled as single beads (W) and other components were not allowed to enter the interior of the NPs. The NP

surface was uniformly coated with hydrophilic beads acting as ligands (L) that interact with the membrane surface.

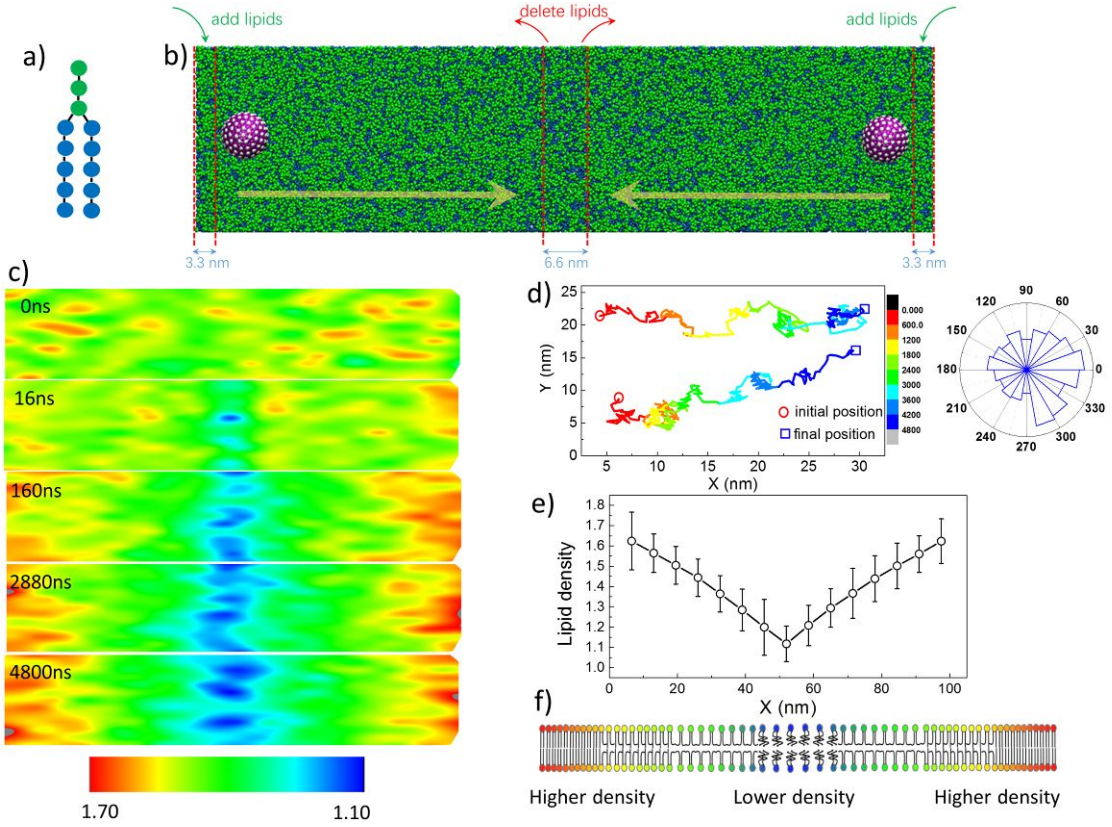

Figure 1. The initial system setup, illustration of the N-varied DPD simulation method, and simulation results of the surface tension propagation. a) The H_3T_5 model of lipid molecule used in our simulations. Headgroup of each lipid is colored in greeen and tails are blue. b) The lipid bilayer membrane with two NPs initially positioned near terminal regions. NPs are colored in purple with surface ligands in white. One central region of width 6.6 nm and two terminal regions of width 3.3 nm are defined as the control regions, where addition and deletion moves of lipids are performed at each time step of the simulation. Flow of lipids under the persistent tension gradient are illustrated by two yellow arrows c) Time sequence of the lipid density distribution along the membrane. d) Moving trajectories of two randomly selected lipids and the average distribution of the turning angle. e) Final distribution of the lipid density along x direction. f) Schematic representation of the membrane in dynamic equilibrium with a linear tension gradient. In the present case, the tension gradient was controlled by setting $\rho_{LNPA}^{low} = 1.1$ and $\rho_{LNPA}^{high} = 1.6$.

Methods. Simulations were performed based on the method of dissipative particle dynamics (DPD), which is a coarse-grained simulation technique with hydrodynamic interactions. In DPD, a small group of atoms is coarse-grained into a single bead to decrease the molecular degree of freedom, thus allowing simulations to be performed in a much longer time than using atomistic models.[22, 24, 31, 37-39] During DPD simulations, the dynamics of each bead was governed by Newton's equation of motion, $dr_i / dt = v_i$ and $dv_i / dt = f_i / m$, similar to the molecular dynamics method. Beads *i* and *j* interact with each other *via* pairwise forces consisting of a conservative force F_{ij}^C, a dissipative force F_{ij}^D, and a random force F_{ij}^R. The total force acting on bead *i* can thus be expressed as $F_i = \sum_{i \neq j} (F_{ij}^C + F_{ij}^D + F_{ij}^R)$. These forces depend on the distance between beads *i* and *j*, and are truncated at a certain cutoff distance r_c. The conservative force is a soft, repulsive force given by $F_{ij}^C = a_{ij}\left(1 - r_{ij}\right)\hat{r}_{ij}$, where a_{ij} is the maximum repulsive force constant between beads *i* and *j*, $r_{ij} = r_j - r_i$ (r_i and r_j are their positions), and $\hat{r}_{ij} = r_{ij} / |r_{ij}|$. Note that in DPD simulations, all interactions are soft repulsive. If an interaction parameter is larger than 25, the corresponding interaction is effectively regarded as repulsive. On the contrary, the interaction is effectively attractive if the parameter is smaller than 25. To model the amphiphilic nature of the lipids, the repulsion parameter between two beads of the same hydrophobicity or hydrophilicity were set to be smaller than that between two beads of which one is hydrophilic and the other hydrophobic. In this system, the interaction parameters between beads of the same type were set to $a_{WW} = a_{HH} = 25$ and $a_{TT} = 15$, and those between different types of beads were $a_{TW} = 80$, $a_{HT} = 50$, and $a_{HW} = 25$. The lower value of 15 was chosen to model the attractive hydrophobic interaction between lipid tails. To represent the adhesive interactions between NPs and membranes, the interaction parameter a_{LH} was varied from 0 to 15 (See Table

S1 for details of the interaction parameters).

The dissipative force and random force act as heat sink and source, respectively, so that their combined effect is a thermostat. The dissipative force has the form $F_{ij}^{D} = -\gamma(1-r_{ij}/r_c)^2(\hat{r}_{ij}\cdot v_{ij})\hat{r}_{ij}$, where γ is the friction coefficient, $v_{ij} = v_j - v_i$ (v_i and v_j are their velocities). The random force is calculated by $F_{ij}^{R} = -\sigma(1-r_{ij}/r_c)^2\theta_{ij}\hat{r}_{ij}$, where σ represents the noise amplitude, and θ_{ij} is an uncorrelated random variable with zero mean and unit variance.

Within each lipid, the interaction between neighboring beads is described by an elastic harmonic force $F_S = K_S(r_{ij} - r_{eq})\hat{r}_{ij}$, where K_S and r_{eq} are the spring constant and the equilibrium bond length, respectively. The numerical values of K_S and r_{eq} used in our simulations are 128 and 0.7, respectively. To maintain the bending rigidity of lipids, the force constraining the variation of the bond angle is given by $F_\varphi = -\nabla U_\varphi$ and $U_\varphi = K_\varphi(1-\cos(\varphi-\varphi_0))$, where φ_0 is set to π and K_φ = 10.0 is the bond bending force constant.

The simulation box size was 160 × 40 × 50 r_c^3, with the periodic boundary conditions applied in all three directions. The time step was set to $\Delta t = 0.02\tau$ to ensure the accurate temperature control over the simulation system.[40] Units in both time and length scales were converted to the SI units by mapping the membrane thickness and the typical diffusion coefficient of lipids, respectively, and we got r_c = 0.65 nm and τ = 0.8 ns.

In investigating the membrane tension propagation and the NP transport, we used a particular variant of DPD method, named the N-varied DPD method. This method was initially developed to study the membrane deformation by anchored proteins,[41] and has been widely used to investigate interactions between membranes and NPs.[31, 33, 42, 43] In this method, the targeted membrane surface tension is controlled by monitoring the lipid number per area (LNPA) in the boundary region, which thus plays the role as a tension buffer. The value of LNPA (denoted as ρ_{LNPA}) is kept

within a defined range ($\rho_{LNPA}^{\min} < \rho_{LNPA} < \rho_{LNPA}^{\max}$) by adding or deleting lipids. Here, we further develop this method by introducing two separate regions, in which the values of ρ_{LNPA} are controlled independently (Figure 1b). The central membrane region along X direction is set to have a lower lipid density (denoted as ρ_{LNPA}^{low}), while two periodically adjacent terminal regions were set to have a higher lipid density (ρ_{LNPA}^{high}). Considering that membranes undergo bending or rupturing under high negative or positive tensions,[44] here we fixed ρ_{LNPA}^{high} to 1.6, and the value of ρ_{LNPA}^{low} was varied from 1.1 to 1.2 and 1.3. In practice, each addition/deletion move of lipids is performed each time step to ensure the constant tension gradient during the simulation.

RESULTS AND DISCUSSION

Surface tension propagation and flow-like lipid diffusion. A rectangular lipid bilayer membrane of 104 nm × 26 nm in lateral size consisting of 9,344 lipid molecules was first constructed and equilibrated for 1.6 μs.[45] The equilibrium value of the lipid density over the entire membrane was thus 1.46, roughly representing a zero membrane surface tension.[44, 45] Then, separate regions respectively locating at the center and two terminals of the membrane were selected and defined as the control regions, where addition and deletion moves of lipids were performed at each time step to generate a persistent tension gradient (Figure 1b). The local lipid densities at the two regions were respectively set as ρ_{LNPA}^{low} = 1.1 and ρ_{LNPA}^{high} = 1.6. Such values were selected to avoid membrane rupturing or bending during the simulation, ensuring that the reduced surface tension can be linearly mapped with the local lipid density, as evidenced by earlier simulations.[41, 44, 45]

Figure 1c shows the evolution of the lipid density distribution (The dynamic process can be found in Video S1), depicting how the surface tension is propagated through the membrane. Initially, the membrane was at equilibrium with its tension being homogeneously distributed (0 ns). Since the targeted lipid densities at the

terminal (1.6) and central (1.1) regions are respectively larger and smaller than the earlier equilibiurm value over the membrane (1.46), lipids were instantly added into and deleted from the two separate regions. Once the local lipid densities were changed, the equilibrium was disturbed to activate a directional flow of lipids from the terminal regions of a larger lipid density to the central region of a smaller density, as expected based on the Fick's law of diffusion.[46] Trajectories of two randomly selected lipids manifested that lipids diffused along the tension gradient in a flowlike pattern,[47] with the diffusion directionality quantified by the average distribution of turning angles of the trajectories (Figure 1d).[22] After a short simulation time (Figure S1), the membrane reached the dynamic equilibrium state, where a linear gradient of the lipid density was maintained (Figure 1e, f). For each position, the local lipid density kept nearly unchanged in the rest of the simulation time (Figure S2), suggesting that the outflow of lipids was compensated by lipids flowing into the region. Under lower tension gradients by increasing the lipid density at the central region from 1.1 to 1.2 and 1.3, the final distribution of lipid density became less steep, albeit with the linearity of the tension gradient being preserved (Figure S3). By comparing trajectories of the same two lipids, it was found that the lipid diffusivity and directionality were both reduced by decreasing the tension gradient (Figure S4).

Once the addition and deletion moves of lipids were turned off to run an equilibrium simulation, the system came into the reverse process, i.e. the generated tension gradient was gradually relieved (Figure S5a). Notably, a lipid density pulse was identified to propagate through the membrane, as reflected in transient distributions of the lipid density along x direction at different time points (Figure S5b). Given symmetry of the membrane along x direction, we extracted both the position and the strength of one pulse activated from the left terminal region of the membrane (Figure S5c, d, see Figure S6 for evolution of the right pulse). In the first 75 ns, the pulse was propelled from the terminal region toward the membrane center (x = 46 nm), with the propelling velocity estimated to ~ 0.6 nm/ns (Figure S5c), close to that measured for propagation of 2D pressure pulses in lipid monolayers by earlier experiments.[17] In this period, we observed a first damping of the pulse followed by an

increase of the pulse strength as two pulses gradually approached each other near the central region (Figure S5d). The strength reached a second peak as two pulses coalesced into a larger one propagated reversely from the membrane center to the terminal regions (t = 100 ns, Figure S5b). Such reciprocating pulse propagation persisted for hundreds of nanoseconds until the pulse was attenuated to be undetected. At the end of the simulation, the system reached the equilibrium state, where surface tension was homogeneously distributed on the membrane (Figure S5a, b).

Translational and rotational motions of NPs on the plasma membrane. The nature of interactions between NPs and plasma membranes is not only determined by intrinsic properties of the NPs,[32, 37, 38, 43, 48-50] but also influenced by properties of the membrane, such as fluidity, rigidity, heterogeneity and curvature.[51-53] For NPs adhering on the membrane with its tension propagated, it was expected that different modes of transport of NPs could endow them with promising applications as local probes of the membrane tension propagation. On the other hand, understanding and control of the NP transport on the mechanically heterogeneous plasma membrane are of importance for their biomedical applications, such as drug delivery, biosensing and diagnosis.[19, 54]

Two NPs initially locating at two terminals of the membrane were controlled to be partially wrapped by the membrane by setting the interaction parameter to 10.0.[55] The time sequence of typical snapshots shows that two NPs were transported synchronously from two terminals of the membrane to gathering at the membrane center (Figure 2a, see Video S2 for detailed process of the NP transport). After reaching the central region, they stopped moving and one NP inserted itself into the membrane to open a hydrophilic pore due to the higher local surface tension (Figure S7).[32] Note that the membrane had a uniform distribution of surface tension before introduction of NPs, after which the addition and deletion moves of lipids were conducted synchronously with transport of NPs. Considering that the final state of membrane with a linear gradient of surface tension can be reached in less than 0.6 μs (Figures S1, S2), we surmise that the effect of membrane initialization on NP transport can be ignored. To provide a detailed insight into the diffusion dynamics of

NPs on the membrane, we calculated the mean square displacement (MSD) of NPs from DPD simulations. We fitted MSD to the scaling t^{α}, yielding the diffusion exponent α. The α under three gradients of membrane surface tension was close to 2.0 (Figure S8), confirming directionality of NP transport on the membrane.

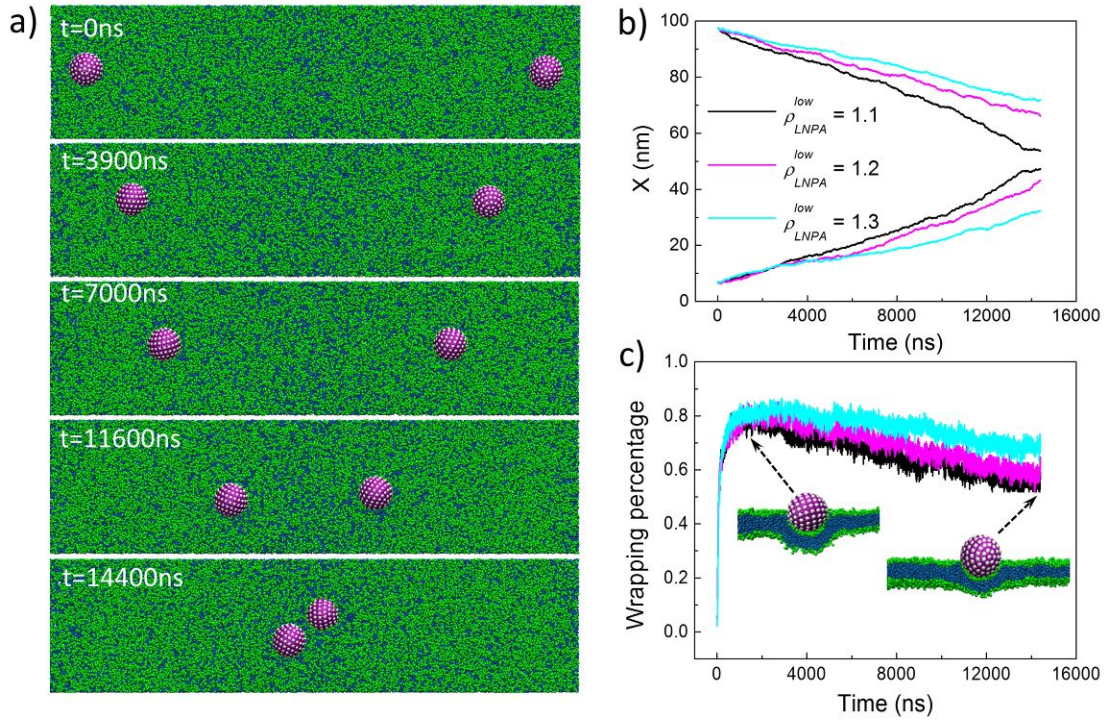

Figure 2. Directional transport of adhesive NPs on the membrane with a constant tension gradient. a) Time sequence of the typical snapshot of two NPs moving synchronously from two terminal regions to the membrane center. b) Time evolutions of the NP position along x direction under three tension gradients. c) Time evolutions of the wrapping percentage of NPs by the membrane under three different tension gradients. The inset of c gives two snapshots from the cross sectional view, showing reduced wrapping extent of NPs as entering the region of a larger surface tension.

Besides directionality of the NP movement, the identified flow-like motion of lipids was enhanced by increasing the tension gradient (Figure S4), thus exerting larger shearing forces to transport NPs at a higher speed on the membrane (Figure 2b). We also observed an acceleration of the NP transport as entering the region of a larger surface tension (Figure 2b), especially under a higher tension gradient (ρ_{LNPA}^{low} = 1.1,

ρ_{LNPA}^{high} = 1.6). To elucidate the reason, we monitored the wrapping process and found a gradual decrease of the wrapping extent for NPs as entering the region of a larger surface tension (Figure 2c). The wrapping related lateral diffusion of NPs on the membrane was observed in previous experiments, and the lower speed of diffusion for fully wrapped NPs was ascribed to the larger membrane drag coefficient.[56] For NPs adhering on the membrane with its surface tension propagated, the case was different as the transport of NPs was not restrained by the membrane but driven by the flow-like motion of surrounding lipids. Besides the wrapping extent that can affect the NP transport, we further calculated the MSD of lipids under different tension gradients (Figure S9). Combining the fitting results of MSD and the trajectories of lipids monitored previously (Figure S4), it can be explained that lipids locating at the membrane of a larger local surface tension diffused at a higher speed, thus accelerating transport of NPs on the membrane. Such speculation was in agreement with previous studies demonstrating that the lipid lateral diffusion coefficient increased with membrane surface tension,[57] as interpreted by the free-area theory.[58]

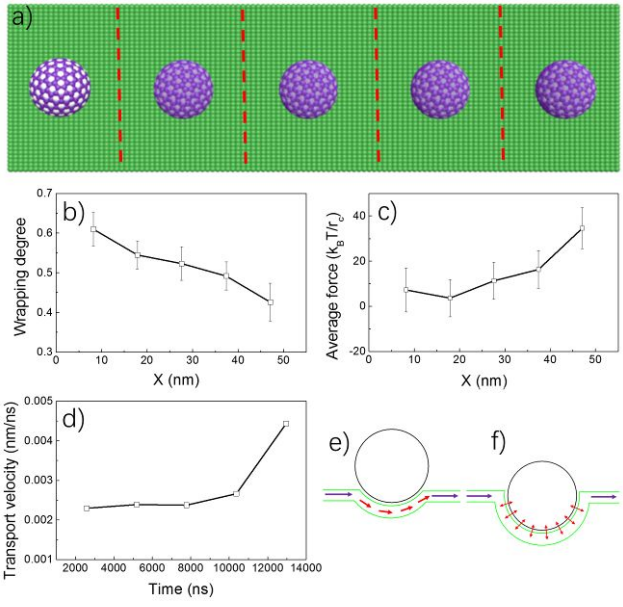

Figure 3. The effect of local membrane surface tension on the transport of NPs on the membrane of its surface tension propagated. a) Schematic depiction of NPs locating at membrane regions of different local surface tensions. NPs were restrained to move along x and y directions, but allowed to rotate and move along z direction. b) The

final wrapping degree as a function of NP position along x direction. c) The average force exerted by flowing lipids on NPs as a function of the NP position. d) The NP transport velocity at discrete time points extracted from Figure 3b. e, f) Schematic illustration of the wrapping dependent NP transport.

To elucidate how the wrapping state influences transport of NPs, five NPs of the same properties were positioned on separate membrane regions of different local surface tensions (Figure 3a). During five independent simulations, the center of mass of each NP was restrained along x and y directions, while both rotation and movement of NPs along the membrane normal direction were allowed to reach the steady wrapping state. As expected, NPs locating at regions of higher surface tensions were finally wrapped by the membrane in less extents (Figure 3b), being consistent with previous simulation studies.[31, 33] After reaching the steady states, we measured the average forces exerted by surrounding lipids on NPs. It appeared that the average force was higher exerted on NPs locating at the regions of larger surface tensions (Figure 3c), in agreement with the higher speed of NP transport as entering the region of larger surface tensions (Figure 3d). It has been proved that when NPs are adhering onto the lipid bilayer membrane, underneath lipids tend to be trapped and behave like a gel phase induced by the NP adhesion (Figure 3e).[59] The trapping can be relieved under lower membrane wrapping degrees to accelerate NP transport driven by lipid flow. For NPs heavily wrapped by the membrane (Figure 3f), the wrapping membrane domain is expected to move along with the NP, thus reducing the speed of NP transport. Such wrapping dependent transport speed was further manifested by positioning NPs at the same membrane region under different adhesion strengths, *i.e.* the average force exerted on NPs decreased with increase of the strength (Figure S10).

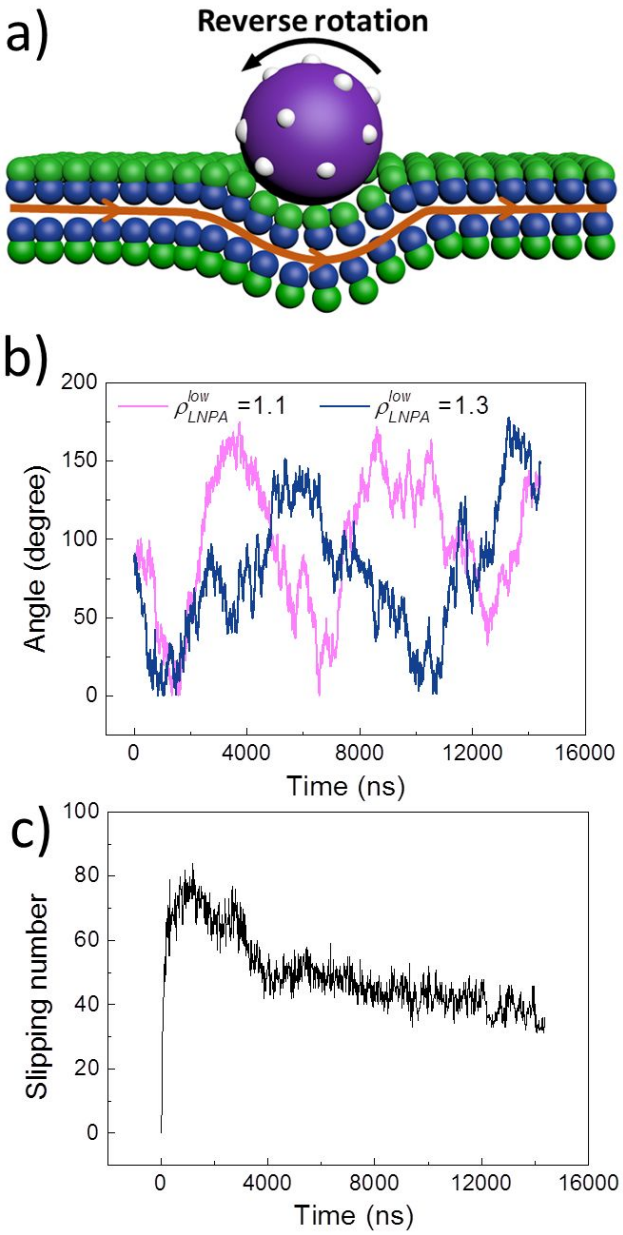

Figure 4. Rotational motion of adhesive NPs on the plasma membrane. a) Schematic depiction of the reverse NP rotation driven by the shearing force exerted by flowing lipids underneath the NP. b) Time evolutions of the rolling angle of NPs on the membrane under two tension gradients. c) Time evolution of the slipping number between the NP and the membrane with a fixed tension gradient of ρ^{low}_{LNPA} = 1.1 and ρ^{high}_{LNPA} = 1.6.

For NPs adhering on the membrane with tension gradients, flowing lipids exert asymmetric shearing forces only on the NP surface in contact with the membrane,

thus driving the rotational NP movement (Figure 4a). Shown in Figure 4b are evolutions of the rotational angle for NPs adhering on the membranes with two tension gradients (Two angles describing the NP rotation are defined in Figure S11). It reads that NPs underwent a continuous reverse rotation being featured by a periodic variation of the angle starting from a sharp decrease. By increasing the lipid density at the central region from 1.1 to 1.3 to decrease the tension gradient, the average rotational speed was reduced from 67 to 47 degree/μs. Such directionality of NP rotation was further verified by the calculated mean square angular displacement, from which the rotational diffusion exponent was fitted close to 2.0 (Figure S12). On account of the NP rotation, the translational motion was somewhat retarded, causing slipping of NPs on the membrane. Figure 4c shows evolution of the slipping number, defined as the number of lipids bound to NPs in the former time step but unbound in the current step. After an initial striking increase *via* membrane wrapping on NPs, the slipping number gradually decreased, reflecting a reduced wrapping extent of the NP as entering the region of a larger surface tension.

Directionality of the NP rotation and the mechanism. We fixed the membrane tension gradient by setting ρ_{LNPA}^{low} = 1.1 and ρ_{LNPA}^{high} = 1.6 and altered the interaction parameter from a_{LH} = 15 to a_{LH} = 5 and a_{LH} = 0 to understand the influence of the membrane adhesion strength in the NP rotation. In reality, the NP-membrane adhesion strength can be increased by varying the ligand type,[60] introducing more surface charges,[61] or increasing the ligand coating density.[30] Identifying the mode of NP rotation requires combining evolutions of both the rolling angle (α, see Figure 5a-c) and the tilt angle (β, see Figure 5d-f). For NPs slightly wrapped by the membrane under a lower adhesion strength (a_{LH} = 15, Figure S13), the rolling angle evolved periodically starting from a decrease from 90º to 0º (Figure 5a), similar to that observed when a_{LH} = 10 (Figure 4b). After a short fluctuation of the rolling angle, during which the tilt angle kept jumping between 0º and 180º (Figure 5d), the rolling angle continued to increase to restart the reverse rotation. As we decreased the

interaction parameter to a_{LH} = 5, no apparent NP rotation was observed in the first 6 μs, being reflected by fluctuations of both the rolling angle and the tilt angle (Figure 5b, e). Upon entering the region of a larger surface tension, a sudden decrease of the rolling angle was observed, reflecting a reverse rotation (Figure 5b). More complex rotational behaviors were observed for NPs being wrapped by the membrane in a higher extent (a_{LH} = 0). In the first stage, the NP underwent a positive rotation, being featured by a first increase of the rolling angle (Figure 5c). However, as the NP entered the region of a larger surface tension to decrease the wrapping extent, a rapid decrease of the rolling angle being accompanied by a sudden increase of the tilt angle reads that the NP contrarily rotated in the reverse direction (Figure 5c, f).

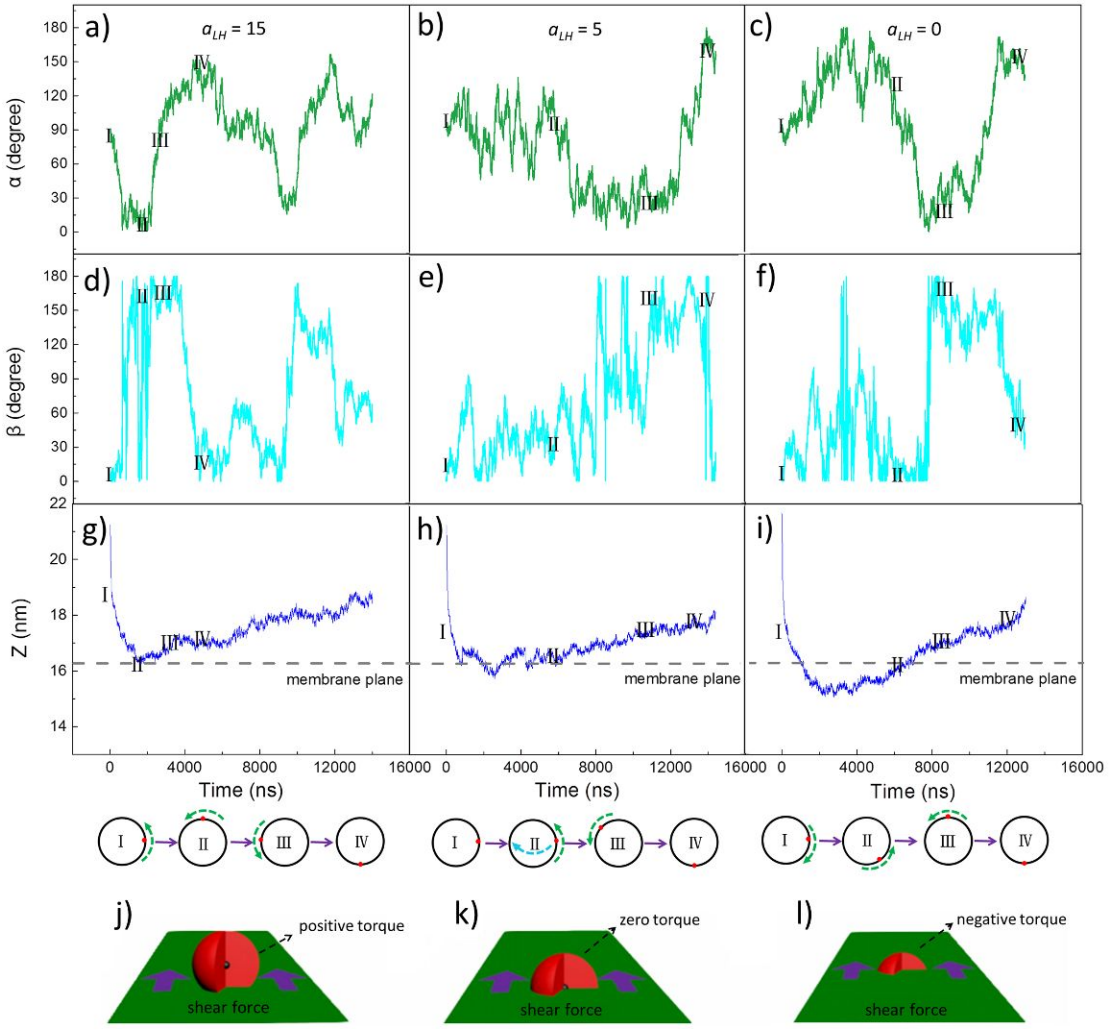

Figure 5. Directionality of the NP rotation determined by the membrane adhesion strength and influenced by the local surface tension. a-c) Time evolutions of the

rolling angle of adhesive NPs. d-f) Time evolutions of the tilt angle of adhesive NPs. g-i) Time evolutions of NP location along membrane normal direction. Below g-i) are several typical states with different rotational modes. The tension gradient is fixed by setting ρ_{LNPA}^{high} = 1.6 and ρ_{LNPA}^{low} = 1.1. The interaction parameter representing the membrane adhesion strength is a_{LH} = 15 (a, d, g), 5 (b, d, h), and 0 (c, f, i), respectively. j-l) Schematic illustration of the torque analysis based on the NP location with respect to the membrane along normal direction. j) Positive torque induced reverse rotation when NPs are slightly wrapped by the membrane. k) Zero torque induced no rotation when half of the NP surface is wrapped by the membrane. l) Negative torque induced positive rotation when most NP surface is wrapped by the membrane.

We make a simple torque analysis to interpret how the mode of NP rotation is sensitive to the membrane interaction state. In our simulations, the membrane wrapping state, or equivalently the NP location with respect to the membrane along normal direction, is not only determined by the membrane adhesion strength, but also influenced by the local membrane surface tension.[53] Figure 5g-i shows evolutions of the NP location under different membrane adhesion strengths. Combining evolutions of the two angles, interestingly, the transient mode of NP rotation is closely related to the NP location. Specifically for the slight wrapping state under a_{LH} = 15, the NP located mostly above the membrane with only bottom of the NP surface getting contact with the membrane (Figure 5g). Thus, the shearing force exerted by flowing lipids underneath the NPs generated a positive torque based on the 'right-hand rule', consequently driving the reverse NP rotation (Figure 5j). If we increased the membrane adhesion strength to make approximately half of the NP surface being immersed into the membrane (Figure 5h), the total shearing force became symmetric to generate a zero torque. Thus, no directional NP rotation took place (Figure 5k). Furthermore, if NPs were wrapped by the membrane in a higher extent, most of the NP surface located below the membrane surface (Figure 5i). Then the generated

torque can be negative to drive the positive NP rotation (Figure 5l). Notably, as NPs moved into the region having a higher surface tension, the wrapping extent was decreased to make NPs emerge from the membrane (Figure 5i). Thus, a positive torque was generated to drive a reverse NP rotation (Figure 5c, f).

CONCLUSIONS

In summary, we have constructed a lipid bilayer membrane with persistent tension gradients, mimicking plasma membranes of migrating cells or cells under constant mechanical stimulation. Using the coarse-grained non-equilibrium membrane simulation method, we investigated dynamic processes of tension propagation, lipid diffusion, and transport of NPs adhering on the membrane. Our results demonstrated that the lipid bilayer membrane can by itself propagate surface tension rapidly to reach a dynamic equilibrium state where surface tension is longitudinally distributed in a linear gradient. The linear tension gradient is maintained essentially by continuous flow-like motions of lipids, which exert shearing forces on adhesive NPs to induce the directional transport. Under certain conditions, the shearing forces can be asymmetric and generate nonzero torques to drive the rotational motion of NPs, with both the sign of the torque and the consequent direction of rotation simply determined by the membrane wrapping state or equivalently the NP location with respect to the membrane along normal direction. Our results provide wide implications for a variety of cellular activities and applications with the transport of NPs involved.

We anticipate that our approach can be extended in several directions to help answer following open questions. First, how the surface tension is propagated on plasma membranes with coexisting domains formed by liquid-ordered and liquid-disordered phases? This is nontrivial because membrane heterogeneity in composition is ubiquitous and of central importance to cellular functioning. Essentially, diffusion of membrane inclusions depends on their size,[62, 63] structural ordering,[64] and aggregating state,[65, 66] thus inducing more complex tension propagation dynamics of the plasma membrane. Second, how the transport of NPs on

plasma membranes is influenced by their physicochemical properties, given that the membrane interaction state of NPs can be modulated by their intrinsic properties? Conversely, how different NPs adhering on, wrapped by, or anchored into the membrane act as obstacles to the tension propagation? Moreover, whether and how NPs bound only on one membrane leaflet affect the flow of lipids in the other leaflet? At last, is there any cooperative or competitive effect during transport of multiple NPs on the membrane?

ASSOCIATED CONTENT

Supporting Information

The Supporting Information is available free of charge on the ACS Publications website

Detailed interaction parameters, membrane tension propagation and the system reaching a dynamic equilibrium state, effect of the tension gradient on the tension propagation, lipid diffusion trajectories and the directionality, propelling evolution of the lipid density pulse activated from terminal regions, gathering of two NPs on the membrane center, mean-square displacement (MSD) for NPs and lipids under different tension gradients, effect of the local membrane surface tension on the transient NP transport, definition of two rotational angles, mean-square angular displacement (MSAD) for NPs, membrane wrapping percentage of NPs under different adhesion strengths (PDF)

The membrane tension propagation reaching a dynamic equilibrium state (AVI)

Directional and rotational motions of NPs on the membrane (AVI)

AUTHOR INFORMATION

Corresponding author

*E-mail: yuett@upc.edu.cn

*E-mail: guoqing.hu@imech.ac.cn

Notes

The authors declare no competing financial interest

ACKNOWLEDGMENTS

This research is financially supported by the National Natural Science Foundation of China (Grant Nos. 31871012, 21303269, 11832017 and 91543125), the Natural Science Foundation of Shandong Province (ZR2018MC004). Part of simulations were performed at the National Supercomputing Center in Shenzhen.

REFERENCES

(1) Lingwood, D.; Simons, K. Lipid rafts as a membrane-organizing principle. *Science* **2010**, *327*, 46-50.

(2) Picas, L.; Rico, F.; Deforet, M.; Scheuring, S. Structural and mechanical heterogeneity of the erythrocyte membrane reveals hallmarks of membrane stability. *ACS Nano* **2013**, *7*, 1054-1063.

(3) Keren, K.; Pincus, Z.; Allen, G. M.; Barnhart, E. L.; Marriott, G.; Mogilner, A.; Theriot, J. A. Mechanism of shape determination in motile cells. *Nature* **2008**, *453*, 475-480.

(4) Houk, A. R.; Jilkine, A.; Mejean, C. O.; Boltyanskiy, R.; Dufresne, E. R.; Angenent, S. B.; Altschuler, S. J.; Wu, L. F.; Weiner, O. D. Membrane tension maintains cell polarity by confining signals to the leading edge during neutrophil migration. *Cell* **2012**, *148*, 175-188.

(5) Keren, K. Cell motility: the integrating role of the plasma membrane. *European Biophys. J.* **2011**, *40*, 1013.

(6) Boulant, S.; Kural, C.; Zeeh, J.-C.; Ubelmann, F.; Kirchhausen, T. Actin dynamics counteract membrane tension during clathrin-mediated endocytosis. *Nat. Cell Biol.* **2011**, *13*, 1124.

(7) Römer, W.; Pontani, L.-L.; Sorre, B.; Rentero, C.; Berland, L.; Chambon, V.; Lamaze, C.; Bassereau, P.; Sykes, C.; Gaus, K. Actin dynamics drive membrane reorganization and scission in clathrin-independent endocytosis. *Cell* **2010**, *140*, 540-553.

(8) Cho, W.; Stahelin, R. V. Membrane-protein interactions in cell signaling and membrane trafficking. *Annu. Rev. Biophys. Biomol. Struct.* **2005**, *34*, 119-151.

(9) Han, B.; Bai, X.-H.; Lodyga, M.; Xu, J.; Yang, B. B.; Keshavjee, S.; Post, M.; Liu, M. Conversion of mechanical force into biochemical signaling. *J. Biol. Chem.* **2004**, *279*, 54793-54801.

(10) Gauthier, N. C.; Masters, T. A.; Sheetz, M. P. Mechanical feedback between membrane tension and dynamics. *Trends Cell Biol.* **2012**, *22*, 527-535.

(11) Lieber, A. D.; Schweitzer, Y.; Kozlov, M. M.; Keren, K. Front-to-rear membrane tension gradient in rapidly moving cells. *Biophys. J.* **2015**, *108*, 1599-1603.

(12) Parsons, J. T.; Horwitz, A. R.; Schwartz, M. A. Cell adhesion: integrating cytoskeletal dynamics and cellular tension. *Nat. Rev. Mol. Cell Biol.* **2010**, *11*, 633-643.
(13) Ranade, S. S.; Syeda, R.; Patapoutian, A. Mechanically activated ion channels. *Neuron* **2015**, *87*, 1162-1179.
(14) Dai, J.; Sheetz, M. In *Regulation of endocytosis, exocytosis, and shape by membrane tension*, Cold Spring Harbor symposia on quantitative biology, Cold Spring Harbor Laboratory Press: 1995; pp 567-571.
(15) Diz-Muñoz, A.; Fletcher, D. A.; Weiner, O. D. Use the force: membrane tension as an organizer of cell shape and motility. *Trends Cell Biol.* **2013**, *23*, 47-53.
(16) Aponte-Santamaría, C.; Brunken, J.; Gräter, F. Stress propagation through biological lipid bilayers in silico. *J. Am. Chem. Soc.* **2017**, *139*, 13588-13591.
(17) Griesbauer, J.; Bössinger, S.; Wixforth, A.; Schneider, M. Propagation of 2D pressure pulses in lipid monolayers and its possible implications for biology. *Phys. Rev. Lett.* **2012**, *108*, 198103.
(18) Reynwar, B. J.; Illya, G.; Harmandaris, V. A.; Müller, M. M.; Kremer, K.; Deserno, M. Aggregation and vesiculation of membrane proteins by curvature-mediated interactions. *Nature* **2007**, *447*, 461-464.
(19) Doane, T. L.; Burda, C. The unique role of nanoparticles in nanomedicine: imaging, drug delivery and therapy. *Chem. Soc. Rev.* **2012**, *41*, 2885-2911.
(20) Petrov, E. P.; Schwille, P. Translational diffusion in lipid membranes beyond the Saffman-Delbrück approximation. *Biophys. J.* **2008**, *94*, L41-L43.
(21) Naji, A.; Atzberger, P. J.; Brown, F. L. Hybrid elastic and discrete-particle approach to biomembrane dynamics with application to the mobility of curved integral membrane proteins. *Phys. Rev. Lett.* **2009**, *102*, 138102.
(22) Chen, P.; Huang, Z.; Liang, J.; Cui, T.; Zhang, X.; Miao, B.; Yan, L.-T. Diffusion and directionality of charged nanoparticles on lipid bilayer membrane. *ACS Nano* **2016**, *10*, 11541-11547.
(23) Shi, X.; von Dem Bussche, A.; Hurt, R. H.; Kane, A. B.; Gao, H. Cell entry of one-dimensional nanomaterials occurs by tip recognition and rotation. *Nat. Nanotechnol.* **2011**, *6*, 714-719.
(24) Yang, K.; Ma, Y.-Q. Computer simulation of the translocation of nanoparticles with different shapes across a lipid bilayer. *Nat. Nanotechnol.* **2010**, *5*, 579-583.
(25) Huang, C.; Zhang, Y.; Yuan, H.; Gao, H.; Zhang, S. Role of nanoparticle geometry in endocytosis: laying down to stand up. *Nano Lett.* **2013**, *13*, 4546-4550.
(26) Gu, Y.; Sun, W.; Wang, G.; Fang, N. Single particle orientation and rotation tracking discloses distinctive rotational dynamics of drug delivery vectors on live cell membranes. *J. Am. Chem. Soc.* **2011**, *133*, 5720-5723.
(27) Yue, T.; Zhang, X.; Huang, F. Molecular modeling of membrane responses to the adsorption of rotating nanoparticles: promoted cell uptake and mechanical membrane rupture. *Soft Matter* **2015**, *11*, 456-465.
(28) Xu, Z.; Yang, Y.; Zhu, G.; Chen, P.; Huang, Z.; Dai, X.; Hou, C.; Yan, L. T. Simulating Transport of Soft Matter in Micro/Nano Channel Flows with Dissipative Particle Dynamics. *Adv. Theory Simul.* **2019**, *2*, 1800160.

(29) Huang, Z.; Chen, P.; Zhu, G.; Yang, Y.; Xu, Z.; Yan, L.-T. Bacteria-Activated Janus Particles Driven by Chemotaxis. *ACS Nano* **2018**, *12*, 6725-6733.
(30) Ding, H. m.; Ma, Y. q. Theoretical and computational investigations of nanoparticle–biomembrane interactions in cellular delivery. *Small* **2015**, *11*, 1055-1071.
(31) Yue, T.; Zhang, X. Cooperative effect in receptor-mediated endocytosis of multiple nanoparticles. *ACS Nano* **2012**, *6*, 3196-3205.
(32) Yue, T.; Zhang, X. Molecular understanding of receptor-mediated membrane responses to ligand-coated nanoparticles. *Soft Matter* **2011**, *7*, 9104-9112.
(33) Mao, J.; Chen, P.; Liang, J.; Guo, R.; Yan, L.-T. Receptor-Mediated Endocytosis of Two-Dimensional Nanomaterials Undergoes Flat Vesiculation and Occurs by Revolution and Self-Rotation. *ACS Nano* **2016**, *10*, 1493-1502.
(34) Apodaca, G. Modulation of membrane traffic by mechanical stimuli. *Am. J. Physiol. - Renal* **2002**, *282*, F179-F190.
(35) Fu, X.; Chen, B.; Tang, J.; Hassan, M. T.; Zewail, A. H. Imaging rotational dynamics of nanoparticles in liquid by 4D electron microscopy. *Science* **2017**, *355*, 494-498.
(36) Groot, R. D.; Rabone, K. Mesoscopic simulation of cell membrane damage, morphology change and rupture by nonionic surfactants. *Biophys. J.* **2001**, *81*, 725-736.
(37) Bai, X.; Xu, M.; Liu, S.; Hu, G. Computational Investigations of the Interaction between the Cell Membrane and Nanoparticles Coated with Pulmonary Surfactant. *ACS Appl. Mater. Interfaces* **2018**, *10*, 20368-20376.
(38) Zhang, L.; Zhao, Y.; Wang, X. Nanoparticle-Mediated Mechanical Destruction of Cell Membranes: A Coarse-Grained Molecular Dynamics Study. *ACS Appl. Mater. Interfaces* **2017**, *9*, 26665-26673.
(39) Li, Y.; Kröger, M.; Liu, W. K. Shape effect in cellular uptake of PEGylated nanoparticles: comparison between sphere, rod, cube and disk. *Nanoscale* **2015**, *7*, 16631-16646.
(40) Vattulainen, I.; Karttunen, M.; Besold, G.; Polson, J. M. Integration schemes for dissipative particle dynamics simulations: From softly interacting systems towards hybrid models. *J. Chem. Phys.* **2002**, *116*, 3967-3979.
(41) Yue, T.; Li, S.; Zhang, X.; Wang, W. The relationship between membrane curvature generation and clustering of anchored proteins: a computer simulation study. *Soft Matter* **2010**, *6*, 6109.
(42) Li, S.; Luo, Z.; Xu, Y.; Ren, H.; Deng, L.; Zhang, X.; Huang, F.; Yue, T. Interaction pathways between soft lipid nanodiscs and plasma membranes: A molecular modeling study. *Biochimica et Biophysica Acta (BBA)-Biomembranes* **2017**, *1859*, 2096-2105.
(43) Guo, R.; Mao, J.; Yan, L.-T. Unique dynamical approach of fully wrapping dendrimer-like soft nanoparticles by lipid bilayer membrane. *ACS Nano* **2013**, *7*, 10646-10653.
(44) Illya, G.; Lipowsky, R.; Shillcock, J. Effect of chain length and asymmetry on material properties of bilayer membranes. *J. Chem. Phys.* **2005**, *122*, 244901.

(45) Shillcock, J. C.; Lipowsky, R. Tension-induced fusion of bilayer membranes and vesicles. *Nat. Mater.* **2005**, *4*, 225-228.
(46) Fick, A. On liquid diffusion. *J. Membrane Sci.* **1995**, *100*, 33-38.
(47) Jeon, J.-H.; Monne, H. M.-S.; Javanainen, M.; Metzler, R. Anomalous diffusion of phospholipids and cholesterols in a lipid bilayer and its origins. *Phys. Rev. Lett.* **2012**, *109*, 188103.
(48) Gao, H.; Shi, W.; Freund, L. B. Mechanics of receptor-mediated endocytosis. *Proc. Natl. Acad. Sci. U. S. A.* **2005**, *102*, 9469-9474.
(49) Vácha, R.; Martinez-Veracoechea, F. J.; Frenkel, D. Receptor-mediated endocytosis of nanoparticles of various shapes. *Nano Lett.* **2011**, *11*, 5391-5395.
(50) Van Lehn, R. C.; Atukorale, P. U.; Carney, R. P.; Yang, Y.-S.; Stellacci, F.; Irvine, D. J.; Alexander-Katz, A. Effect of particle diameter and surface composition on the spontaneous fusion of monolayer-protected gold nanoparticles with lipid bilayers. *Nano Lett.* **2013**, *13*, 4060-4067.
(51) Agudo-Canalejo, J.; Lipowsky, R. Adhesive nanoparticles as local probes of membrane curvature. *Nano Lett.* **2015**, *15*, 7168-7173.
(52) Van Lehn, R. C.; Ricci, M.; Silva, P. H.; Andreozzi, P.; Reguera, J.; Voïtchovsky, K.; Stellacci, F.; Alexander-Katz, A. Lipid tail protrusions mediate the insertion of nanoparticles into model cell membranes. *Nat. Commun.* **2014**, *5*, 4482.
(53) Yue, T.; Zhang, X.; Huang, F. Membrane monolayer protrusion mediates a new nanoparticle wrapping pathway. *Soft Matter* **2014**, *10*, 2024-2034.
(54) Davis, M. E.; Shin, D. M. Nanoparticle therapeutics: an emerging treatment modality for cancer. *Nat. Rev. Drug Discov.* **2008**, *7*, 771-782.
(55) Yue, T.; Xu, Y.; Sun, M.; Zhang, X.; Huang, F. How tubular aggregates interact with biomembranes: wrapping, fusion and pearling. *Phys. Chem. Chem. Phys.* **2016**, *18*, 1082-1091.
(56) Shigyou, K.; Nagai, K. H.; Hamada, T. Lateral Diffusion of a Submicrometer Particle on a Lipid Bilayer Membrane. *Langmuir* **2016**, *32*, 13771-13777.
(57) Reddy, A. S.; Warshaviak, D. T.; Chachisvilis, M. Effect of membrane tension on the physical properties of DOPC lipid bilayer membrane. *Biochimica et Biophysica Acta (BBA)-Biomembranes* **2012**, *1818*, 2271-2281.
(58) Galla, H.-J.; Hartmann, W.; Theilen, U.; Sackmann, E. On two-dimensional passive random walk in lipid bilayers and fluid pathways in biomembranes. *J. Membr. Biol.* **1979**, *48*, 215-236.
(59) Wang, B.; Zhang, L.; Bae, S. C.; Granick, S. Nanoparticle-induced surface reconstruction of phospholipid membranes. *Proc. Natl. Acad. Sci. U. S. A.* **2008**, *105*, 18171-18175.
(60) Schubertová, V.; Martinez-Veracoechea, F. J.; Vácha, R. Influence of ligand distribution on uptake efficiency. *Soft Matter* **2015**, *11*, 2726-2730.
(61) Villanueva, A.; Cañete, M.; Roca, A. G.; Calero, M.; Veintemillas-Verdaguer, S.; Serna, C. J.; del Puerto Morales, M.; Miranda, R. The influence of surface functionalization on the enhanced internalization of magnetic nanoparticles in cancer cells. *Nanotechnology* **2009**, *20*, 115103.
(62) Guigas, G.; Weiss, M. Size-dependent diffusion of membrane inclusions.

Biophys. J. **2006**, *91*, 2393-2398.
(63) Weiß, K.; Neef, A.; Van, Q.; Kramer, S.; Gregor, I.; Enderlein, J. Quantifying the diffusion of membrane proteins and peptides in black lipid membranes with 2-focus fluorescence correlation spectroscopy. *Biophys. J.* **2013**, *105*, 455-462.
(64) Lindblom, G.; Orädd, G. Lipid lateral diffusion and membrane heterogeneity. *Biochimica et Biophysica Acta (BBA)-Biomembranes* **2009**, *1788*, 234-244.
(65) Cicuta, P.; Keller, S. L.; Veatch, S. L. Diffusion of liquid domains in lipid bilayer membranes. *J. Phys. Chem. B* **2007**, *111*, 3328-3331.
(66) Horton, M. R.; Höfling, F.; Rädler, J. O.; Franosch, T. Development of anomalous diffusion among crowding proteins. *Soft Matter* **2010**, *6*, 2648-2656.

TOC graphic